NeuroImage: Clinical 35 (2022) 103030

Contents lists available at ScienceDirect

NeuroImage: Clinical

journal homepage: www.elsevier.com/locate/ynicl

Diffusion tractography of superior cerebellar peduncle and dentatorubrothalamic tracts in two autopsy confirmed progressive supranuclear palsy variants: Richardson syndrome and the speech-language variant

Rodolfo G. Gatto [a], Peter R. Martin [b], Farwa Ali [a], Heather M. Clark [a], Joseph R. Duffy [a], Rene L. Utianski [a], Hugo Botha [a], Mary M. Machulda [c], Dennis W. Dickson [d], Keith A. Josephs [a], Jennifer L. Whitwell [e,*]

[a] Department of Neurology, Mayo Clinic, Rochester, MN, USA
[b] Department of Quantitative Health Sciences, Mayo Clinic, Rochester, MN, USA
[c] Department of Psychiatry and Psychology, Mayo Clinic, Rochester, MN, USA
[d] Department of Neuroscience, Mayo Clinic, Jacksonville, FL, USA
[e] Department of Radiology, Mayo Clinic, Rochester, MN, USA

ARTICLE INFO

Keywords:
Progressive supranuclear palsy
MRI
Diffusion tensor imaging
Tractography
Superior cerebellar peduncle
Dentato-rubro-thalamic tract
Richardson's syndrome

ABSTRACT

Background: Progressive supranuclear palsy (PSP) is a 4-repeat tauopathy with neurodegeneration typically observed in the superior cerebellar peduncle (SCP) and dentatorubrothalamic tracts (DRTT). However, it is unclear how these tracts are differentially affected in different clinical variants of PSP.

Objectives: To determine whether diffusion tractography of the SCP and DRTT can differentiate autopsy-confirmed PSP with Richardson's syndrome (PSP-RS) and PSP with predominant speech/language disorder (PSP-SL).

Methods: We studied 22 autopsy-confirmed PSP patients that included 12 with PSP-RS and 10 with PSP-SL. We compared these two groups to 11 patients with autopsy-confirmed Alzheimer's disease with SL problems, i.e., logopenic progressive aphasia (AD-LPA) (disease controls) and 10 healthy controls. Whole brain tractography was performed to identify the SCP and DRTT, as well as the frontal aslant tract and superior longitudinal fasciculus. We assessed fractional anisotropy and mean diffusivity for each tract. Hierarchical linear modeling was used for statistical comparisons, and correlations were assessed with clinical disease severity, ocular motor impairment, and parkinsonism. DRTT connectomics matrix analysis was also performed across groups.

Results: The SCP showed decreased fractional anisotropy for PSP-RS and PSP-SL and increased mean diffusivity in PSP-RS, compared to controls and AD-LPA. Right DRTT fibers showed lower fractional anisotropy in PSP-RS and PSP-SL compared to controls and AD-LPA, with PSP-RS also showing lower values compared to PSP-SL. Reductions in connectivity were observed in infratentorial DRTT regions in PSP-RS vs cortical regions in PSP-SL. PSP-SL showed greater abnormalities in the frontal aslant tract and superior longitudinal fasciculus compared to controls, PSP-RS, and AD-LPA. Significant correlations were observed between ocular motor impairment and SCP in PSP-RS ($p = 0.042$), and DRTT in PSP-SL ($p = 0.022$). In PSP-SL, the PSP Rating Scale correlated with the SCP ($p = 0.045$) and DRTT ($p = 0.008$), and the Unified Parkinson's Disease Rating Scale correlated with the DRTT ($p = 0.014$).

Conclusions: Degeneration of the SCP and DRTT are diagnostic features of both PSP-RS and PSP-SL and associations with clinical metrics validate the role of these tracts in PSP-related clinical features, particularly in PSP-SL.

* Corresponding author at: Department of Radiology, Mayo Clinic, 200 1st St SW, Rochester MN 55905, USA.
E-mail address: whitwell.jennifer@mayo.edu (J.L. Whitwell).

https://doi.org/10.1016/j.nicl.2022.103030
Received 20 January 2022; Received in revised form 27 April 2022; Accepted 29 April 2022
Available online 11 May 2022

1. Introduction

Progressive supranuclear palsy (PSP) is a neurodegenerative disorder typically characterized by ocular motor impairment and early postural instability with falls (Steele et al., 1964). This typical presentation of PSP is described as PSP-Richardson's syndrome (PSP-RS) (Höglinger et al., 2017; Litvan et al., 1996; Williams et al., 2005). However, it has been recognized for many years that PSP can also present with progressive speech and language deficits, particularly apraxia of speech (Josephs et al., 2005; Josephs et al., 2006). This clinical variant of PSP has been added to the recent clinical diagnostic criteria for PSP as PSP with predominant speech/language disorder (PSP-SL) (Höglinger et al., 2017). Patterns of neurodegeneration differ between these two clinical variants of PSP (PSP-RS and PSP-SL), although there is some overlap (Whitwell et al., 2020; Whitwell et al., 2021). Whereas PSP-SL has been associated with involvement of the premotor cortex (Whitwell et al., 2013; Whitwell et al., 2019), PSP-RS is typically associated with atrophy of the midbrain, basal ganglia, and frontal lobe (Whitwell et al., 2017). Imaging studies have also shown that atrophy (Josephs et al., 2008; Paviour et al., 2005) and diffusion signal changes (Kataoka et al., 2019; Kataoka et al., 2008) in the superior cerebellar peduncle (SCP) are characteristic features of PSP-RS.

Diffusion MRI (dMRI) measures water diffusion in the brain and allows for the specific assessment of the integrity of white matter and directional water diffusion along white matter tracts. dMRI studies have demonstrated degeneration of the SCP in PSP-RS (Agosta et al., 2012a; Knake et al., 2010; Nicoletti et al., 2008; Whitwell et al., 2011a; Whitwell et al., 2014; Whitwell et al., 2021) and shown that degeneration of the SCP is related to clinical outcomes in PSP-RS, including disease severity and ocular motor impairment (Whitwell et al., 2019). Abnormalities have been observed throughout the dentatorubrothalamic (DRTT) tract which involves connections from the cerebellar dentate through the SCP to the red nucleus, and up to the thalamus and the cortex, in PSP-RS (Whitwell et al., 2011a). An additional advantage of dMRI is that it allows the mapping of specific tracts that roughly represent white matter bundles (Jeurissen et al., 2019). Such local fiber orientations can then be pieced together to infer long-range pathways linking proximal or remote areas of the brain, a process frequently named fiber tracking or fiber tractography (Mori and van Zijl, 2002) Tractography studies have characterized the structural integrity from large fascicular bundles, like the DRTT (Kwon et al., 2011; Mollink et al., 2016), and demonstrated abnormalities in the DRTT tract in PSP-RS (Seki et al., 2018; Surova et al., 2015).

In contrast to PSP-RS, patients clinically diagnosed with PSP-SL show atrophy of the premotor and motor regions of the frontal lobe, with less involvement of infratentorial regions (Whitwell et al., 2013; Whitwell et al., 2019). Using dMRI, we observed greater degeneration of the SCP in PSP-RS compared to PSP-SL (Whitwell et al., 2021), suggesting that involvement of the SCP varies across PSP variants. However, no studies have utilized tractography to assess the degree of involvement of the SCP or DRTT in PSP-SL. Furthermore, the pathology underlying PSP-SL is heterogeneous, with PSP pathology only observed in approximately 67% of patients clinically diagnosed with PSP-SL (Hokelekli et al., 2022; Josephs et al., 2021), and from the Hokelekli study we focus on a subgroup of PSP-SL patients who underwent neuroimaging studies. Hence, autopsy-confirmed cases are needed to assess how SCP and DRTT integrity relates to PSP pathology.

In this study, we applied dMRI tractography to determine specific features of the SCP and DRTT that allow the characterization of autopsy-confirmed PSP in patients who initially presented as PSP-RS and PSP-SL. Our working hypothesis is that the integrity of the SCP and DRTT can potentially differentiate these two PSP variants and that these tracts may have different relationships to clinical outcomes in these PSP variants.

2. Methods

2.1. Participants

PSP patients for this study were prospectively recruited by the Neurodegenerative Research Group (NRG) from the Department of Neurology at the Mayo Clinic, Rochester, Minnesota between 02/2010 and 12/2018. All participants underwent detailed neurological, neuropsychological, and speech and language assessments and cognitive screen, as well as a 3 T MRI protocol that included dMRI. To be included in this study, patients must have received a clinical diagnosis of possible or probable PSP-RS or possible PSP-SL during life according to recent diagnostic criteria (Höglinger et al., 2017), have died and undergone a brain autopsy, and received an autopsy diagnosis of PSP (Hauw et al., 1994). A total of 12 autopsy-confirmed PSP-RS patients and 11 autopsy-confirmed PSP-SL patients were identified. These groups were compared to two control cohorts that had undergone identical neuroimaging: 1) a disease control cohort that consisted of 10 patients with speech/language problems but with AD pathology at autopsy (Montine et al., 2012) (diagnosed clinically with logopenic progressive aphasia (AD-LPA) (Botha et al., 2015; Gorno-Tempini et al., 2008)) and 2) 10 cognitively unimpaired control participants. Healthy controls were included if they did not have any complaints of cognitive, motor, or behavioral abnormalities and performed normally on the Montreal Cognitive Assessment Battery (MoCA) ($\geq$26) and the Hoehn and Yahr scale (score of 0). The study was approved by the Mayo Clinic IRB and informed consent was obtained from all participants.

2.2. Imaging analysis

2.2.1. Data acquisition and preprocessing

All patients and controls underwent a standardized MRI protocol on a 3 T GE scanner. The imaging protocol included a 3D Magnetization Prepared Rapid Acquisition Gradient-Echo (MPRAGE) sequence as well as a dMRI sequence with a spin-echo single shot Echo Planar Imaging (EPI) sequence. Each dMRI scan included a set of two diffusion-weighted values: b = 0 and b = 1000 s/mm^2. Forty-one diffusion gradients were included on each shell. The in-plane resolution was 1.36 mm scanned with 2.0 mm isotropic voxels, with a slice thickness of 2.7 mm. Images were corrected for head motion, Eddy current, and susceptibility artifact distortion using standard algorithms extensively described elsewhere (Andersson et al., 2018; Andersson and Sotiropoulos, 2016). Additionally, diffusion data was checked by an automatic quality control routine to ensure its accuracy and avoid outliers (Schilling et al., 2019b).

A diffusion tensor model was estimated and subsequently used to calculate fractional anisotropy (FA) and mean diffusivity (MD) employing an open-source software (DSI studio) [https://dsi-studio.labsolver.org] (Yeh, 2021). Incorporated algorithms on this software allow checking the accuracy and reliability of the data [SRC fiber quality control] (Yeh et al., 2019b). Seed points were manually selected based on a balance given by input data and an optimal number of the tract by visual inspections. Our basic criteria applied to mean this balancing technique for selecting the number of seed points (Cheng et al., 2012; Zajac et al., 2017). Regions where the mean FA was below 0.2, were removed from consideration. Datasets from each group were non-linearly co-registered using a probabilistic brain atlas via an iterative group-wise registration algorithm and spatially normalized into a Montreal Neurological Institute (MNI) space to generate an averaged diffusion template (1 mm isotropic). On occasions, due to gross anatomical degeneration/deformations, manual correction, and realignment of grey and white matter regions of interest were performed by experienced users familiar with neuroanatomical landmarks.

2.2.2. Tractography reconstructions

Tractography was calculated for the SCP and DRTT, as well as for four association tracts. The third inner branch of the superior

Table 1
Demographic and clinical features of the groups.

	Control (N = 10)	PSP-RS (N = 12)	PSP-SL (N = 10)	AD-LPA (N = 11)	p value
Female sex	4 (40%)	6 (50%)	6 (60%)	8 (73%)	0.481
Education	14 (12, 16)	14 (12, 16)	16 (15, 20)	16 (15, 17)	0.117
Age onset, y		65 (60, 66)	73 (65, 74)	64 (60, 68)	0.089
Age MRI, y	63 (60, 67)	68 (63, 71)	78 (72, 82)	72 (63, 74)	0.011
Onset to MRI, y		4 (3, 4)	6 (5, 8)	4 (3, 5)	0.004
MRI to death, y		2 (2, 3)	4 (3, 4)	4 (4, 6)	< 0.001
MoCA	28 (24, 29)	22 (21, 27)	22 (18, 26)	17 (14, 24)	0.021
PSIS		4 (3, 4)	1 (1, 3)	0 (0, 0)	0.006
MDS-UPDRS III		47 (46, 54)	32 (25, 68)	4 (2, 6)	< 0.001
PSP Rating Scale		43 (38, 49)	32 (18, 49)	4 (4, 4)	0.127
WAB-AQ			90 (80, 96)	82 (76, 86)	0.172
ASRS		2 (2, 3)	25 (23, 31)	3 (2, 4)	0.002

Abbreviations: MoCA, Montreal Cognitive Assessment; PSP-RS, Progressive Supranuclear Palsy, Richardson's syndrome-; PSP-SL, Progressive Supranuclear Palsy with predominant Speech/Language disorder; AD-LPA, Alzheimer's disease with Logopenic Progressive Aphasia; PSIS, PSP Saccadic Impairment Scale; MDS-UPDRS III, Movement Disorder Society-sponsored revision of the -Unified Parkinson's Disease Rating Scale; WAB-AQ, Western Aphasia Battery Aphasia Quotient; ASRS, Apraxia of Speech Rating Scale total score.

longitudinal fasciculus and the frontal aslant tract was assessed since they are frequently affected in patients with PSP-RS and patients with apraxia of speech/agrammatic aphasia (Josephs et al., 2013). We also included for negative comparison purposes the middle longitudinal and inferior longitudinal fasciculi, as these are less involved in PSP. A whole-brain deterministic fiber tracking algorithm (with augmented tracking strategies) was used to improve reproducibility (Yeh et al., 2013). An anatomical tractography atlas was used to map all tracts (Abos et al., 2019; Yeh et al., 2018). A seeding region was placed at a standardized white matter region of interest. The anisotropy threshold, angular threshold, and step size were randomly selected by the software. Tracks with a length shorter than 3 mm or longer than 5,000 mm were discarded. A total of 500,000 seeds were placed with a distance voxel tolerance of 32 mm.

2.2.3. *Correlative tractography & tractograms*

Conveying quantitative measures to the reconstructed tractography streamlines, numerical quantities (average numerical values and variance) from derived diffusivity parameters (FA or MD) can be mapped to points on the reconstructed streamlines and displayed on the fiber tracts themselves. To estimate the false discovery rate (FDR), a total of 4000 randomized permutations were applied to the group label to obtain the null distribution of the track length. An FDR threshold of 0.05 was used to select tracks. A non-parametric Spearman's correlation was used to derive the correlations between DTI parameters and clinical scores. A T-score threshold of 2.5 was assigned and tracked (Yeh et al., 2016b). We derived correlational tractograms to represent negative or positive associations between FA and clinical parameters (Yeh et al., 2016a), and map spatial correlations (Chamberland et al., 2019). Clinical scales used included the PSP Saccadic Impairment Scale (PSIS) (Whitwell et al., 2011c), PSP Rating Scale (Golbe and Ohman-Strickland, 2007; Hall et al., 2015), and the Movement Disorders Society-sponsored revision of the Unified Parkinson's Disease Rating Scale part III for motor impairment (MDS-UPDRS- III) (Kroonenberg et al., 2006).

2.2.4. *Connectomics & connectivity matrix*

Structural connectivity matrixes from each PSP group were calculated by grey matter region-of-interest connected along the tract

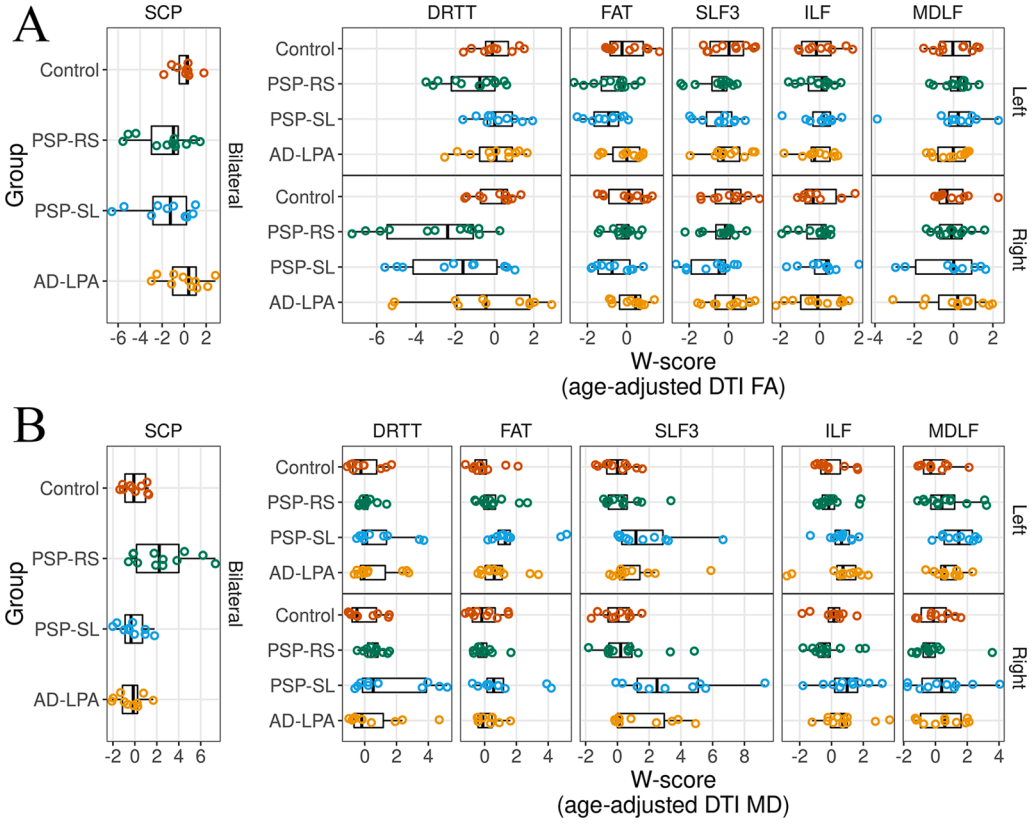

Fig. 1. Boxplots of fractional anisotropy (FA) (A) and mean diffusivity (MD) (B) W-scores in control, PSP-RS, PSP-SL, and AD-LPA groups across multiple white matter tracts. Measurements in this figure are a weighted average across hemispheres within a tract. Abbreviations: DRTT, dentatorubrothalamic tract, SCP, superior cerebellar tract; FAT, frontal Aslant tract; ILF, inferior longitudinal fascicle; MDLF, middle longitudinal fasciculi; SLF-3, superior longitudinal fasciculi (inner portion); PSP-RS, Progressive Supranuclear Palsy, Richardson's syndrome; PSP-SL, Progressive Supranuclear Palsy with predominant Speech/Language disorder; AD-LPA, Alzheimer's disease with Logopenic Progressive Aphasia.

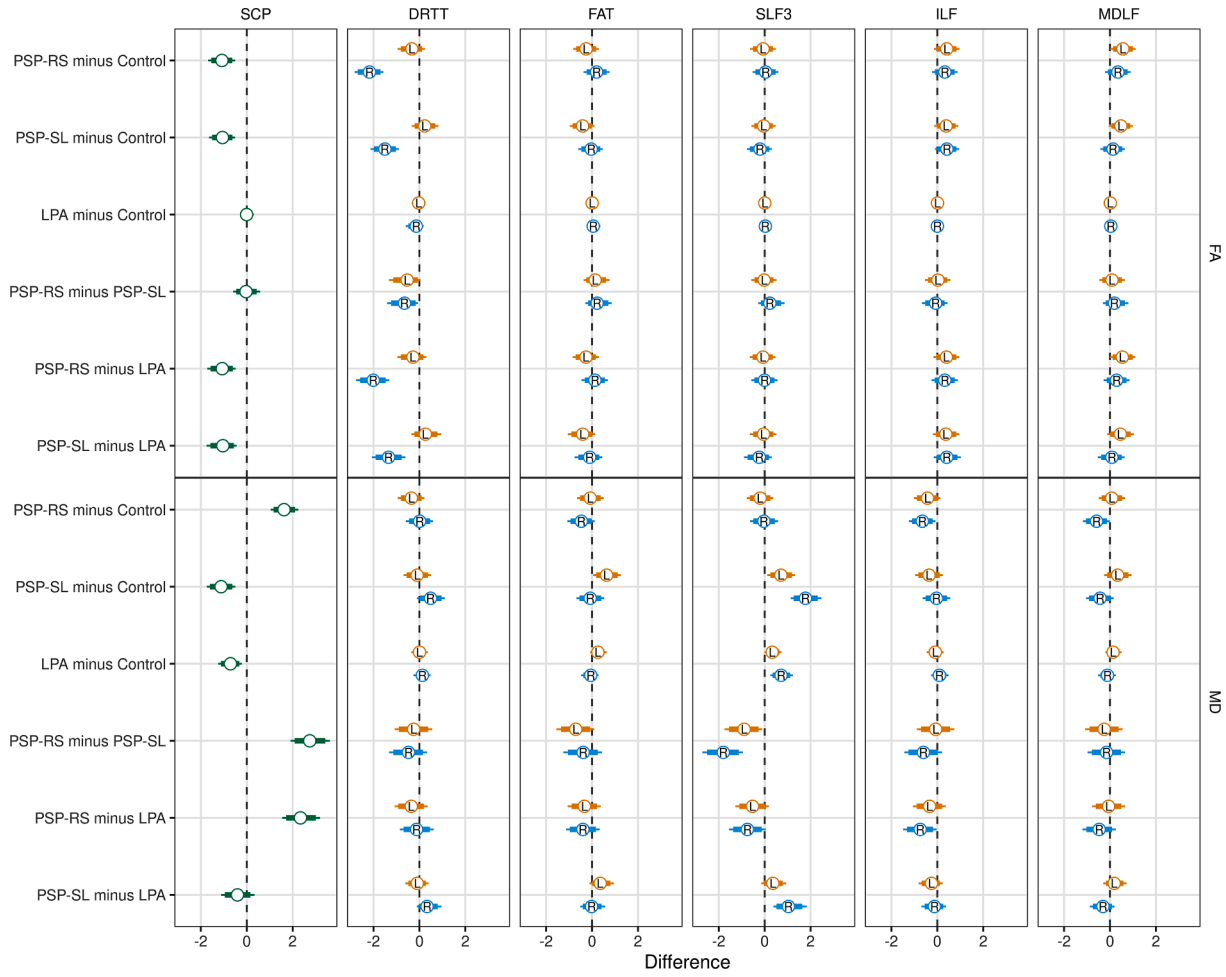

Fig. 2. Estimated differences between groups in fractional anisotropy (FA) and mean diffusivity (MD) W-scores based on posterior distributions from the hierarchical models. Each median difference is denoted by a circle and hemisphere is denoted by color and letter; yellow and "L" indicate left while blue and "R" indicate right. The SCP is bilateral, is colored green, and has no letter overlaid on the median estimate. Behind each circle are whiskers denoting confidence intervals. The thick whiskers denote an 80% interval showing when neither whisker crosses the zero-line, moderate evidence (posterior probability > 0.90) of a difference between groups. The thin whiskers represent a 90% interval, and the thin whisker not crossing the zero line indicates strong evidence (posterior probability > 0.95) of a difference between groups. Abbreviations: DRTT, dentato-rubro-thalamic tract, SCP, superior cerebellar peduncle; FAT, frontal Aslant tract; ILF, inferior longitudinal fascicle; MDLF, middle longitudinal fasciculi; SLF-3, superior longitudinal fasciculi (inner portion); PSP-RS, Progressive Supranuclear Palsy, Richardson's syndrome; PSP-SL, Progressive Supranuclear Palsy with predominant Speech/Language disorder; AD-LPA, Alzheimer's disease with Logopenic Progressive Aphasia. (For interpretation of the references to color in this figure legend, the reader is referred to the web version of this article.)

(DRTT). Due to the crossing nature of the DRTT, areas from the cerebellum III, IV, V, VI, VIII, X, cerebellum crus I & II, as well as the dentate nucleus (left side) were included on the ipsilateral side (Kwon et al., 2011). The red nucleus, the thalamic and frontal areas (frontal superior 2, frontal superior medial, precentral postcentral) represented the DRTT contralateral side. Both SCP and DRTT fiber streams were calculated using the dMRI settings as previously described. Comparisons of PSP-RS and PSP-SL were established by connectivity strength on the right DRTT by Pearson's correlations within the average matrix.

2.3. Statistical analysis

All statistical analyses were performed using R statistical software (R Core Team, 2020) version 4.0.3 and GraphPad prism 9.0 for windows (San Diego, CA, USA, www. graphpad.com). To determine whether there were group-wise differences across tracts and hemispheres, we used an age-adjusted FA or MD score as the outcome predicted by the group within each tract and hemisphere. To achieve this, first W-scores were generated by fitting, within tract and hemisphere, linear regression in controls predicting average FA and MD, respectively, by an intercept and age term. Then these model fits were used to predict expected FA and MD values for each case. Following, standardized residuals were created by subtracting the expected value from the observed value, dividing by the standard deviation of the residuals of controls used in each original linear model. These plots serve to visualize our data as well as check for outliers. A Bayesian hierarchical model prospectively manages the problem of multiple comparisons and allows us to include multiple measurements per person in a single model (Greenland, 2000). These models are used for the analysis of individual tracts and hemispheres in each DTI contrast, FA, or MD, predicting W-score, age-adjusted FA or MD respectively, using the following terms: (i) an overall intercept, (ii) tract-and-side specific estimates for each group (i.e., we are pooling some information across groups within tract-and-side), and (iii) overall intercept per person (this adjusts for a person being generally "high" or generally "low" overall). After the model was fit using Markov-Chain Monte Carlo simulation, posterior probabilities were calculated from the set of posterior samples (a common method of model fitting in the Bayesian paradigm). Posterior probabilities > 0.90 were considered moderate evidence of a difference and either posterior probabilities > 0.95 (1/20 chance of being wrong) or > 0.99 (1/100 chance of being wrong) as strong evidence, based on clinical preference. Correlations between DTI parameters and collected clinical variables

Table 2
Hierarchical Linear Model - Posterior probabilities.

Contrast	Tract	Side	PSP-RS vs Control	PSP-SL vs Control	AD-LPA vs Control	PSP-RS vs PSP-SL	PSP-RS vs AD-LPA	PSP-SL vs AD-LPA
FA	SCP	Bilateral	0.999	0.999	0.521	0.538	0.998	0.998
	DRTT	Left	0.825	0.743	0.599	0.936	0.781	0.754
		Right	> 0.999	> 0.999	0.752	0.966	> 0.999	0.998
	FAT	Left	0.779	0.901	0.520	0.666	0.782	0.889
		Right	0.726	0.548	0.686	0.768	0.652	0.620
	SLF3	Left	0.584	0.555	0.518	0.530	0.591	0.560
		Right	0.547	0.736	0.618	0.766	0.506	0.755
	ILF	Left	0.888	0.889	0.533	0.533	0.879	0.863
		Right	0.838	0.908	0.506	0.599	0.833	0.888
	MDLF	Left	0.955	0.929	0.561	0.617	0.946	0.905
		Right	0.847	0.661	0.645	0.746	0.810	0.596
MD	SCP	Bilateral	> 0.999	0.998	0.993	> 0.999	> 0.999	0.824
	DRTT	Left	0.841	0.607	0.511	0.698	0.792	0.636
		Right	0.512	0.912	0.739	0.833	0.608	0.889
	FAT	Left	0.585	0.962	0.896	0.924	0.779	0.898
		Right	0.907	0.588	0.607	0.777	0.816	0.529
	SLF3	Left	0.711	0.976	0.944	0.969	0.891	0.882
		Right	0.538	> 0.999	0.994	> 0.999	0.939	0.996
	ILF	Left	0.894	0.844	0.669	0.557	0.787	0.815
		Right	0.971	0.541	0.671	0.891	0.958	0.664
	MDLF	Left	0.593	0.827	0.752	0.696	0.556	0.753
		Right	0.954	0.887	0.697	0.620	0.860	0.847

Dark orange shading indicates strong evidence of a difference (posterior probability > 0.95) and lighter shading indicates moderate evidence of a difference (posterior probability > 0.90). **Abbreviations:** PSP-RS, Progressive Supranuclear Palsy, Richardson's syndrome; PSP-SL, Progressive Supranuclear Palsy with predominant Speech/Language disorder; AD-LPA, Alzheimer's disease with Logopenic Progressive Aphasia; DRTT; dentato-rubro-thalamic tract; SCP, superior cerebellar tract; FAT, frontal Aslant tract; ILF, inferior longitudinal fascicle; MDLF, middle longitudinal fasciculi; SLF-3, superior longitudinal fasciculi (inner portion).

from PSP subjects were performed using Spearman's rank correlation coefficient. Coefficients of correlation (r) > 0.5 were interpreted as strongly correlated (Schober et al., 2018). Specifically, correlations between FA and MD from each tract were explored with PSIS, PSP Rating scale, MDS-UPDRS III, MoCA, and MMSE. Our correlation analyses didn't account for age because they are marginal and the lower sample size of each group, ignoring the effects of age in the results of our correlations. We used Benjamini-Hochberg method test (Benjamini and Hochberg, 1995) for multiple comparison corrections.

3. Results

3.1. Demographic and clinical group comparisons

The four groups did not differ in terms of sex or education, but there was a difference in age at scan, with the oldest age observed in PSP-SL and in time from MRI to death with the shortest median time between MRI and death in the PSP-RS group (Table 1). The groups also differed on the MoCA, with the lowest scores observed in AD-LPA.

3.2. Tractography of the SCP and DRTT

Initial FA and MD data for each tract and study group are shown in plots from Fig. 1. Pair-wise group differences in W-scores with posterior probabilities from the hierarchical model are shown in Fig. 2 and Table 2. Inter-group comparisons performed using the hierarchical linear model revealed both moderate evidence (posterior probability > 0.90) and strong evidence (posterior probabilities > 0.95) for differences across tracts. In the SCP, there was strong evidence of lower FA in both PSP-RS and PSP-SL compared to AD-LPA and controls, with no differences observed between PSP-RS and PSP-SL. However, MD was only increased in PSP-RS compared to controls, with PSP-RS showing strong evidence for greater MD compared to PSP-SL and AD-LPA. For the DRTT, there was strong evidence of lower FA in the right DRTT in PSP-RS and PSP-SL compared to controls and AD-LPA, with moderate-strong evidence that PSP-RS had lower FA than PSP-SL. There was no strong evidence for group differences in MD for the DRTT.

From each group, our combined SCP tractography demonstrated a significant reduction of fibers in both PSP-RS and PSP-SL (Supplementary Fig. 1). Based on an initial equal number of seeds, our DRTT reconstructions showed a significant decrease in the number of DRTT stems in the PSP-RS group compared to the PSP-SL group (Fig. 3).

3.3. Connectomics of the DRTT

Connectomics analysis inter-region Pearson correlation coefficients for the DRTT are shown in Fig. 4. The PSP-RS group showed negative correlations within infratentorial cerebellar regions and negative correlations between infratentorial regions and supratentorial regions, including the thalamus and frontal regions. In contrast, the PSP-SL group showed negative correlations within supratentorial regions, and between supratentorial and infratentorial regions. No negative correlations were identified in controls or AD-LPA.

3.4. Tractography of association tracts

In the frontal aslant tract, there was strong evidence for greater MD and moderate evidence for lower FA on the left in PSP-SL compared to controls (Table 2 **and** Fig. 2). There was also moderate evidence for greater MD in the left frontal aslant tract in PSP-SL compared to PSP-RS and moderate evidence for lower MD in the right frontal aslant tract in PSP-RS compared to controls. No group differences were observed for FA in the superior longitudinal fasciculus. However, there was strong evidence for greater MD in the superior longitudinal fasciculus in PSP-SL compared to controls, PSP-RS, and AD-LPA (Fig. 2 and Table 2). There was also moderate-strong evidence for greater MD in the superior

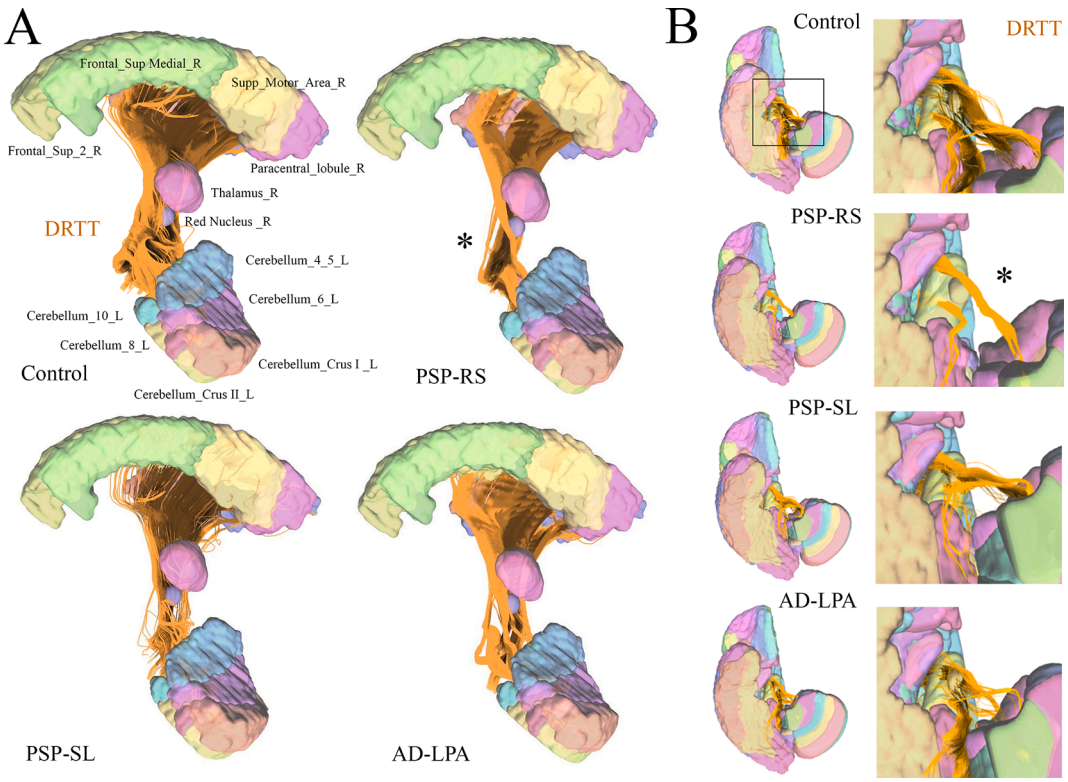

Fig. 3. Tractography reconstructions from dentatorubral thalamic tract (DRTT) among different study groups. Lateral (Fig. 3A) and inferior (Fig. 3B) of the right drtt connecting the left cerebellum to the right cortex view are displayed for comparison. Note that seeding and reconstruction of DRTT fibers not only display crossing fibers but also a recognized population of homolateral fibers. Note the significant white matter differences between PSP-RS (*) and PSP-SL groups. Abbreviations: PSP-RS, Progressive Supranuclear Palsy, Richardson's syndrome; PSP-SL, Progressive Supranuclear Palsy with predominant Speech/Language disorder; AD-LPA, Alzheimer's disease with Logopenic Progressive Aphasia.

longitudinal fasciculus in AD-LPA compared to controls and PSP-RS, particularly on the right.

3.5. Correlations with clinical metrics

Correlations between FA in the SCP and the PSIS were stronger in the PSP-RS group ($r = 0.59$, $p = 0.042$) compared to the PSP-SL group ($r = 0.37$, $p = 0.28$), showing lower FA with worsening ocular motor impairment in PSP-RS. On the other hand, a stronger association was observed between FA and PSIS on DRTT fibers from the PSP-SL group ($r = 0.84$, $p = 0.022$) **(**Fig. 5**A)**. Significant correlations between SCP and DRTT FA and the PSP rating scale were observed in the PSP-SL group ($r = 0.64$, $p = 0.045$ for CSP and $r = 0.78$, $p = 0.008$, for DRTT), but not in PSP-RS (Fig. 6**A**). Similarly, a significant correlation was observed between FA in the DRTT and MDS-UDPRS III in the PSP-SL group ($r = 0.74$, $p = 0.014$). Correlations with the MDS-UPDRS III occurred in the most anterior portion of the DRTT tractograms in PSP-SL (Fig. 6**B**). However after using Benjamini-Hochberg method test, none of these correlations survive the corrections.

4. Discussion

In this study, we confirmed the involvement of the SCP and DRTT in PSP-RS and further demonstrated that these tracts are also degenerated in PSP-SL, implying a specific PSP-related pattern of local vulnerability. However, our measures could also differentiate PSP-RS and PSP-SL, with greater SCP and DRTT degeneration observed in PSP-RS and additional degeneration of association tracts usually impaired in language pathology, including the frontal aslant tract and superior longitudinal fasciculus, in PSP-SL. There was also evidence of different patterns of structural connectivity of the DRTT, with PSP-RS showing greater disruption of connections in infratentorial regions and PSP-SL showing greater disruption in supratentorial regions. Lastly, diffusivity was not affected in the SCP and DRTT in AD-LPA.

Our results for PSP-RS concur with previous tractography studies that have demonstrated degeneration of the DRTT, as well as the SCP (Kataoka et al., 2019; Sakamoto et al., 2021; Seki et al., 2018), though our study demonstrates the involvement of these tracts in autopsy-confirmed PSP cases. The results also demonstrate that these tracts are involved in PSP-SL, again utilizing cases with PSP at autopsy, suggesting that SCP and DRTT degeneration may be a common biomarker of PSP pathology. We previously found relative sparing of the SCP in PSP-SL, although that study utilized region-of-interest-based analyses rather than tractography, and the cohort lacked autopsy confirmation (Whitwell et al., 2021). Patients with PSP-SL can also have corticobasal degeneration at autopsy (Hokelekli et al., 2022), and hence it would be reasonable to conclude that the diffusion signal in our previous study was weakened by the inclusion of corticobasal degeneration. Brainstem involvement is greater in speech-language patients with PSP compared to those with corticobasal degeneration (Josephs et al., 2021). No previous study has assessed the DRTT in PSP-SL, and here we demonstrate that the DRTT is involved in PSP-SL, although to a lesser extent than is seen in PSP-RS. Furthermore, we found different patterns of structural connectivity breakdowns, with PSP-RS showing greater breakdowns in infratentorial regions and their connections, while PSP-SL showed greater breakdowns in supratentorial regions and their connections. This would fit with the fact that PSP-SL is associated with a shift in the distribution of tau pathology, with greater cortical pathology and less involvement of the brainstem compared to PSP-RS (Josephs et al., 2005; Whitwell et al., 2020). Furthermore, PSP-related features and involvement of the brainstem develop later in the disease course in PSP-SL (Whitwell et al., 2019). Also consistent with this shift in pathology

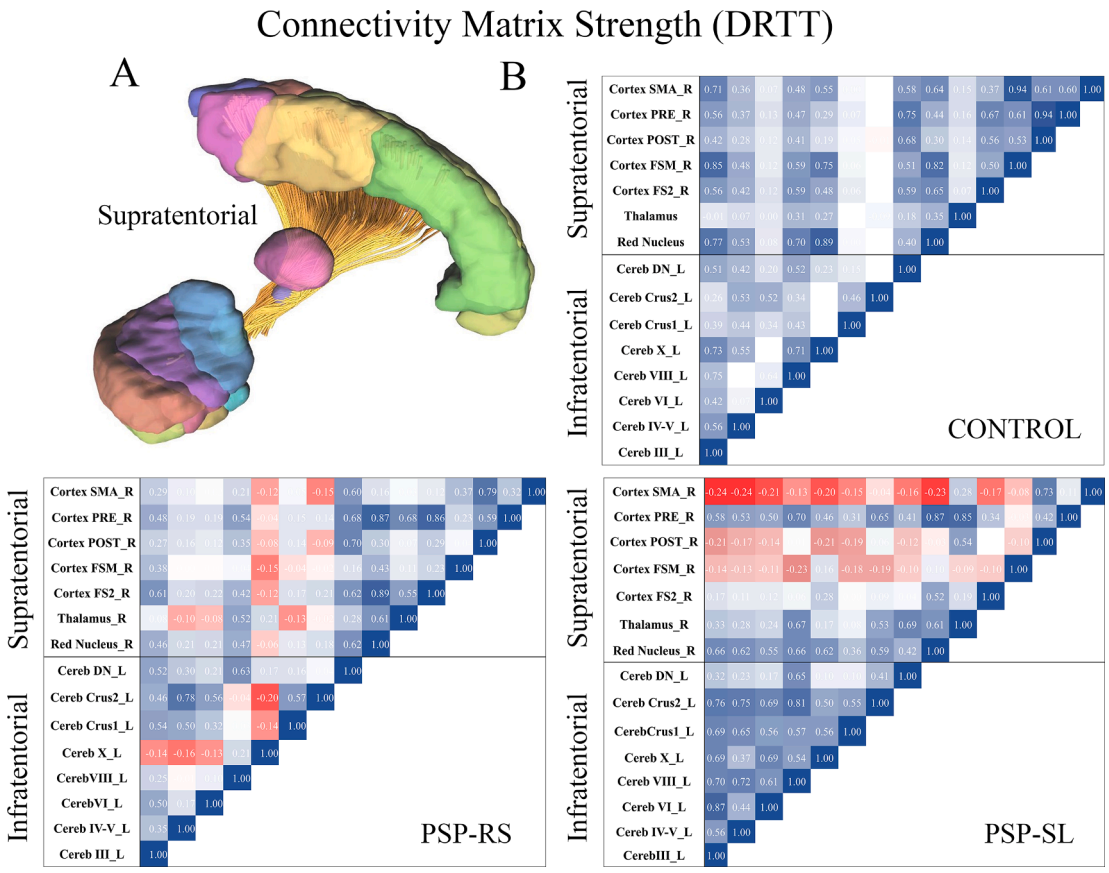

Fig. 4. DRTT matrix connectivity strength (Pearson correlation coefficient), indicating positive correlation (blue) and negative correlations (red) from interlinks across different grey matter areas. The PSP-RS group showed negative correlations within infratentorial regions and negative correlations between infratentorial and supratentorial regions. In contrast, areas of negative correlation were exclusively allocated within cortical regions in the PSP-SL group demonstrating that the changes in connectivity strength in this variant are topographically different and more connected to the symptomatology of this PSP phenotype. Abbreviations: PSP-RS, Progressive Supranuclear Palsy, Richardson's syndrome; PSP-SL, Progressive Supranuclear Palsy with predominant Speech/Language disorder; R, right; L, left; Cerebellar areas 3; IV-V, Cerebellar area 4–5; VI, cerebellar area 6; XIII, cerebellar area 8; X, Cerebellar area 10; Crus1, Cerebellar Crus area 1; Crus2, Cerebellar Crus Area 2; DN, Dentate Nucleus; FS2, Frontal Superior Medial Gyrus; FSM, Frontal Superior Motor area; POST, postcentral area; PRE, Precentral area; SMA, Supplementary Motor Area. (For interpretation of the references to color in this figure legend, the reader is referred to the web version of this article.)

was the fact that the PSP-SL group showed greater degeneration of the frontal aslant tract and superior longitudinal fasciculus compared to PSP-RS. Regarding right DRTT diffusivities in the PSP-SL group, connectomics studies have demonstrated an asymmetric distribution of cerebello-thalamic connections favorable to the right side of the cerebellum (Ou et al., 2021). Given that the distribution of the ascending crossing fibers projecting to the contralateral motor/premotor and prefrontal regions of the frontal lobe are dependent on thalamic-cerebral connections it is possible for a preferential disconnection at the infratentorial levels in the PSP-SL groups. Another possibility is that microstructural changes in the DRTT are indirectly related to language impairment, but play a more important role in the extrapyramidal symptomatology of PSP (Hana et al., 2016).

The frontal aslant tract has previously been shown to be associated with speech and language features, including fluency (Catani et al., 2013; Dick et al., 2019) which suggests that involvement of this tract is related to the speech and language abnormalities observed in PSP-SL. Previous studies have found that the superior-medial (supracallosal) portion of the left frontal superior longitudinal fasciculus is also associated with speech pathology (Davtian et al., 2008; Madhavan et al., 2014). These two tracts were involved to a greater degree in PSP-SL compared to AD-LPA, although AD-LPA also showed abnormalities in the superior longitudinal fasciculus compared to controls and PSP-RS. These findings concord with previous studies that found abnormalities in the superior longitudinal fasciculus in patients with agrammatic primary progressive aphasia, which overlaps clinically with PSP-SL (Agosta et al., 2012b; Galantucci et al., 2011; Whitwell et al., 2010), and in patients with LPA (Galantucci et al., 2011; Madhavan et al., 2016; Mahoney et al., 2013). The third segment of the superior longitudinal fasciculus is more involved in agrammatic primary progressive aphasia compared to LPA (Galantucci et al., 2011). The inferior and middle longitudinal fasciculi were preserved in both PSP groups and showed increased MD compared to AD-LPA and controls. Although the reason for this increase is unclear, it may be related to the capacity of the brain to compensate for the cellular loss by neuroplasticity mechanisms, rewiring, and masking regional white matter changes during the evolution of the disease (Gatto, 2020).

The underlying representation of diffusivity parameters remains uncertain, it is possible to interpret FA as a general indicator of axonal degeneration, and assume MD as a measure of interstitial diffusivity, (Gatto et al., 2021). In the context of PSP, the decrease in FA could be part of the tau-driven pathology mechanism, whereas MD findings may be related to underlying gliotic infiltrative and neuroinflammatory processes, (Ling et al., 2016; Pascual et al., 2021) (Whitwell et al., 2011b), or the presence of brain atrophy on the macro-pathological (ie millimeter) level. As the differences between groups in FA were greater than differences in MD it is possible that the two PSP variants are not equally affected by tau aggregation, with a different distribution across the neuroaxis determining the different connectivity changes and clinical presentations.

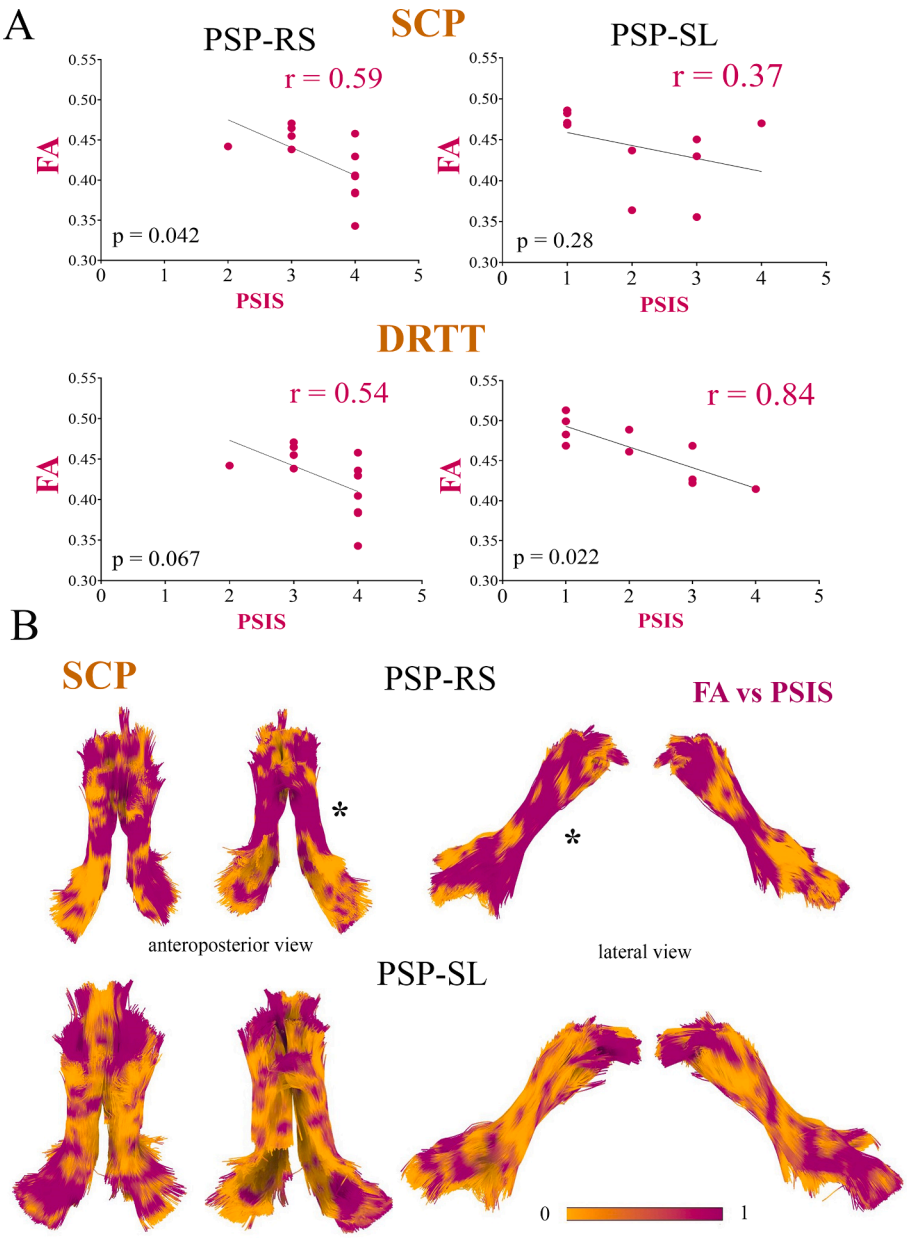

Fig. 5. Correlations between FA and the PSP Saccadic Impairment (PSIS) scale. Fig.5A - Correlative analysis between fractional anisotropy (FA) from the SCP and PSP Saccadic Impairment Scale (PSIS), showed a stronger association within the PSP-RS group. A similar correlation in WM microstructure was seen by the dentate-rubro-thalamic tract (DRTT) in PSP-RS but with a larger association in the PSP-SL group Fig. 5B – Tractograms localizing the t-scores association between FA and PSIS show different distribution patterns between average skeletons from PSP-RS and PSP-SL subjects.

We also found relationships between tract integrity and clinical features in our cohort that differed between the two PSP variants. The severity of ocular motor impairment was associated with degeneration of the SCP in the PSP-RS group, and the DRTT in the PSP-SL group. This may imply that eye movement anomalies in PSP-RS patients tend to occur due to the involvement of impaired conjugate gaze systems within midbrain regions where the oculomotor nucleus is located. Conversely, the association of DRTT and ocular motor impairment in PSP-SL may represent impairment of the supranuclear oculomotor component due to a cortical and ocular motor disconnection through nerves that control eye movement (Karatas, 2009; Morris et al., 1999). Diffusion metrics from the SCP have previously been shown to correlate to ocular motor impairment (Zhang et al., 2016) and disease severity (Agosta et al., 2014; Whitwell et al., 2011c) in PSP-RS. Some imaging studies have also shown that SCP atrophy correlates with disease duration (Tsuboi et al., 2003). The DRTT was also associated with disease severity measured by the PSP Rating Scale and parkinsonism measured by the MDS-UPDRS III in PSP-SL, but not in PSP-RS. The fact that the DRTT, but not the SCP, correlated with PSP features in PSP-SL may reflect the greater involvement of the cortex in PSP-SL. We found that correlations between FA and the MDS-UDPRS III were predominantly located in the anterior (frontal) position of the DRTT. Therefore, the selective involvement of DRTT axons in PSP variants could explain the severity of different PSP features.

The detection of microstructural diffusivity changes does not necessarily guarantee anatomical changes in dMRI tractography reconstructions (Thomas et al., 2014). As an example, increasing MD changes detected in SCP from PSPRS did not show ostensible changes in the fiber tract reconstructions. This could reinforce the theory that micro diffusivity changes captured by MD are more related to extracellular compartment anomalies that could be an independent finding of axonal degeneration not detected by the tractography reconstructions. Another possible explanation could reside in the difference between the voxel size and biological ultrastructure scales, which makes it extremely challenging to detect early WM changes, even with high magnetic fields (Gatto et al., 2018; Gatto et al., 2019). Therefore, partial volume effects need to be considered when diffusion MRI and other imaging techniques need to be compared (Alexander et al., 2001).

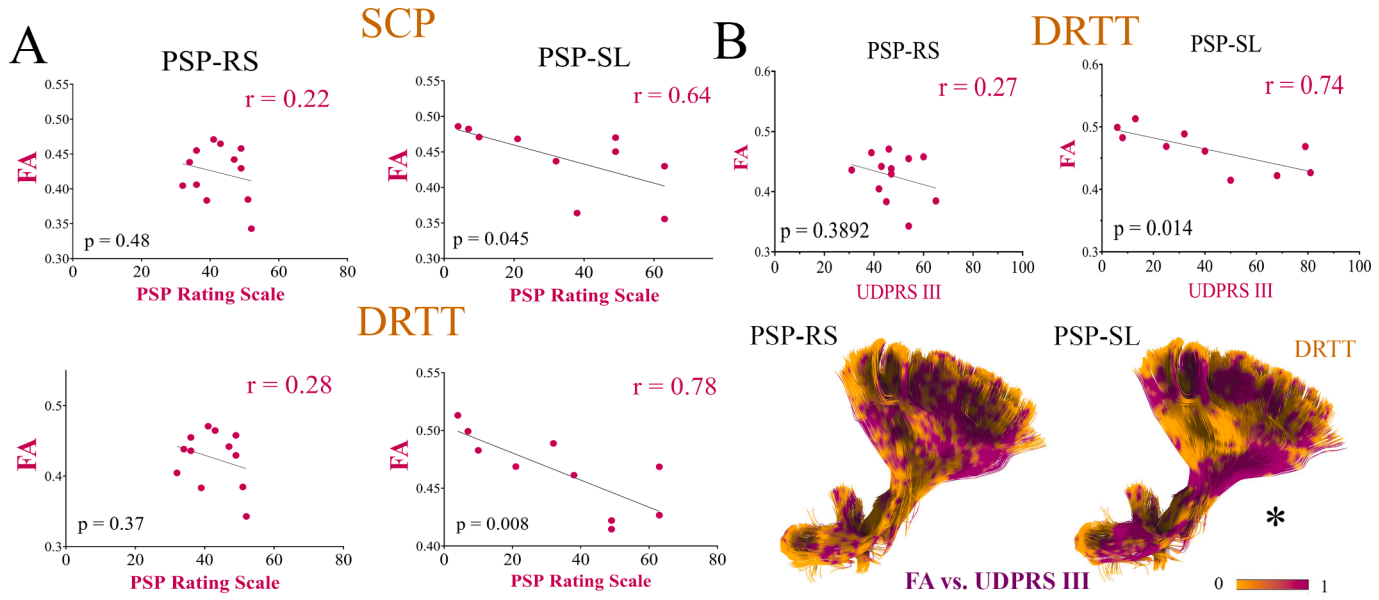

Fig. 6. Correlations between FA and the PSP Rating Scale and UPDRS III. Fig. 6A Initial correlative analysis- SCP & DRTT between fractional anisotropy (FA) and PSP rating Scale by Spearman rank-order correlations coefficients (r) have shown high values in the PSP-SL groups. Fig. 6B - Similar larger r values were also seen from correlations between FA and the motor examination (Part III) of the Unified Parkinson's Disease Rating Scale (UDPRS III). Note that DRTT tractograms representing the negative t-distribution between FA and UDPRS III also display higher association in the PSP-RS group, particularly located in the anterior sections of the tract (*).

The accuracy of our tractography reconstructions is intrinsically limited due to brain tissue loss and significant anatomical distortions making it a challenging task in some cases to manually adjust each atlas-based anatomical region of interest and avoid misrepresentations. Although new automatic techniques have been developed to remove false connections using topology-informed pruning to improve tractography accuracy (Yeh et al., 2019a) its potential application in the neurodegenerative field remains uncertain due to the possibility of removing true deficient connections and eliminating valuable information. Although dMRI can perform DRTT reconstructions with acceptable accuracy compared to histological techniques (Mollink et al., 2016), tractography has limited capabilities when facing complex microarchitectural patterns (Campbell and Pike, 2014; Schilling et al., 2019a; Thomas et al., 2014). This is particularly relevant due to the crossing nature of DRTT fibers. To address these limitations, recent work has applied fixel-based analysis, a technique that facilitates fiber tract-specific statistical analysis in the investigation of diffusivity properties of DRTT fibers from PSP patients (Sakamoto et al., 2021). Along those lines, whole-voxel reconstruction techniques like generalized q-sampling imaging (Tuch, 2004) have been postulated as an ideal technique to provide additional intra-voxel information and improvements in anatomical accuracy (Yeh et al., 2010)'. Therefore, the limitations of dMRI-based tractography reconstructions (Bonilha et al., 2015) and their influence on the representation of brain connectivity need to be considered. Future studies will be needed to investigate if alternative diffusion methods can enhance brain connectivity and network analytics, as well as to better differentiate PSP variants. The number of participants in our cohort was also relatively small due to the requirement of autopsy confirmation, and hence our findings will need to be replicated in larger studies to determine generalizability. Regarding our statistical analysis, we chose a priori to correct for age in our hierarchical model and not sex given our limited sample size and the fact that age, more than sex, was deemed more likely to affected associations. Although the gender ratios did not differ significantly, there was an imbalance which could have influenced the dMRI findings. Future studies with larger cohorts will be needed to assess gender effects on diffusivity in these disorders. We were also aware of the disparities in terms of disease duration across groups. However, correcting for these differences is not straight forward. The PSP-SL group had a longer time from onset to MRI but also a longer total duration from onset to death compared to PSP-RS. In fact, the MRI scans were performed at a similar relative time in the total disease course in both groups. PSP-SL patients typically have a longer disease course than PSP-RS patients because they have relatively isolated speech and language deficit for on average 5–6 years before developing clinical features of PSP correcting for disease (Whitwell et al., 2019).This is an important factor to be considered in the interpretation of the correlative data analysis for each PSP subgroup. We also noted that in the PSP-RS group, there was only a trend in the correlations between DRTT's FA and UPDRS-motor scale III & PSP rating scales. This is likely due to a limited range of scores on both scales.

We intended to use the AD-LPA group as a positive disease control group in which we did not expect to see changes in the SCP and DRTT. This helps to support the specificity of the findings to our PSP groups and illuminate potential methodological confounds. As part of our future directions, we consider comparing PSP-SL to other groups, such as nfvPPA patients with underlying TDP-43 pathology, although we do not have yet a large enough cohort of such patients.

5. Conclusions

This study showed that degeneration of the SCP and DRTT occur in both PSP-RS and PSP-SL and are associated with clinical features in these patients. The assessment of microstructural changes by combining dMRI metrics and tractography techniques has improved the neuroimaging characterization of PSP variants. However, considerations regarding the different age of prevalence on each PSP subgroup, and proper statistical corrections, need to be considered in the interpretation of the results. The use of dMRI metrics in the context of clinical characterization may be considered a potentially useful approach to support PSP neuropathological findings and a valuable diagnostic tool in the study of imaging PSP biomarkers in this patient population.

Uncited references

CRediT authorship contribution statement

Rodolfo G. Gatto: Conceptualization, Formal analysis, Methodology, Visualization, Writing – original draft, Writing – review & editing.

Peter R. Martin: Data curation, Formal analysis, Methodology, Visualization, Writing – review & editing. **Farwa Ali:** Investigation, Writing – review & editing. **Heather M. Clark:** Investigation, Writing – review & editing. **Joseph R. Duffy:** Investigation, Writing – review & editing. **Rene L. Utianski:** Investigation, Writing – review & editing. **Hugo Botha:** Writing – review & editing. **Mary M. Machulda:** Investigation, Writing – review & editing. **Dennis W. Dickson:** Investigation, Writing – review & editing. **Keith A. Josephs:** Conceptualization, Funding acquisition, Investigation, Supervision, Writing – review & editing. **Jennifer L. Whitwell:** Conceptualization, Funding acquisition, Investigation, Supervision, Writing – review & editing.

Declaration of Competing Interest

The authors declare that they have no known competing financial interests or personal relationships that could have appeared to influence the work reported in this paper.

Acknowledgments

This study was funded by the National Institutes of Health, grant numbers R01-NS89757, R01-DC12519, R01-DC14942, RF1-NS112153, and R01-DC010367.

Disclosures

The authors have no financial disclosures to report.

Data availability

Data collected for this study are available upon reasonable direct request to the corresponding author.

Appendix A. Supplementary data

Supplementary data to this article can be found online at https://doi.org/10.1016/j.nicl.2022.103030.

References

Abos, A., Segura, B., Baggio, H.C., Campabadal, A., Uribe, C., Garrido, A., Camara, A., Munoz, E., Valldeoriola, F., Marti, M.J., Junque, C., Compta, Y., 2019. Disrupted structural connectivity of fronto-deep gray matter pathways in progressive supranuclear palsy. Neuroimage Clin 23, 101899.

Agosta, F., Galantucci, S., Svetel, M., Lukić, M.J., Copetti, M., Davidovic, K., Tomić, A., Spinelli, E.G., Kostić, V.S., Filippi, M., 2014. Clinical, cognitive, and behavioural correlates of white matter damage in progressive supranuclear palsy. J. Neurol. 261 (5), 913–924.

Agosta, F., Pievani, M., Svetel, M., Ječmenica Lukić, M., Copetti, M., Tomić, A., Scarale, A., Longoni, G., Comi, G., Kostić, V.S., Filippi, M., 2012a. Diffusion tensor MRI contributes to differentiate Richardson's syndrome from PSP-parkinsonism. Neurobiol. Aging 33 (12), 2817–2826.

Agosta, F., Scola, E., Canu, E., Marcone, A., Magnani, G., Sarro, L., Copetti, M., Caso, F., Cerami, C., Comi, G., Cappa, S.F., Falini, A., Filippi, M., 2012b. White matter damage in frontotemporal lobar degeneration spectrum. Cereb. Cortex 22, 2705–2714.

Alexander, A.L., Hasan, K.M., Lazar, M., Tsuruda, J.S., Parker, D.L., 2001. Analysis of partial volume effects in diffusion-tensor MRI. Magn. Reson. Med. 45 (5), 770–780.

Andersson, J.L.R., Graham, M.S., Drobnjak, I., Zhang, H., Campbell, J., 2018. Susceptibility-induced distortion that varies due to motion: Correction in diffusion MR without acquiring additional data. Neuroimage 171, 277–295.

Andersson, J.L.R., Sotiropoulos, S.N., 2016. An integrated approach to correction for off-resonance effects and subject movement in diffusion MR imaging. Neuroimage 125, 1063–1078.

Benjamini, Y., Hochberg, Y., 1995. Controlling the False Discovery Rate: A Practical and Powerful Approach to Multiple Testing. J. Roy. Stat. Soc.: Ser. B (Methodol.) 57 (1), 289–300.

Bonilha, L., Gleichgerrcht, E., Fridriksson, J., Rorden, C., Breedlove, J.L., Nesland, T., Paulus, W., Helms, G., Focke, N.K., 2015. Reproducibility of the Structural Brain Connectome Derived from Diffusion Tensor Imaging. PLoS One 10, e0135247.

Botha, H., Duffy, J.R., Whitwell, J.L., Strand, E.A., Machulda, M.M., Schwarz, C.G., Reid, R.I., Spychalla, A.J., Senjem, M.L., Jones, D.T., Lowe, V., Jack, C.R., Josephs, K.A., 2015. Classification and clinicoradiologic features of primary progressive aphasia (PPA) and apraxia of speech. Cortex 69, 220–236.

Campbell, J.S., Pike, G.B., 2014. Potential and limitations of diffusion MRI tractography for the study of language. Brain Lang. 131, 65–73.

Catani, M., Mesulam, M.M., Jakobsen, E., Malik, F., Martersteck, A., Wieneke, C., Thompson, C.K., Thiebaut de Schotten, M., Dell'Acqua, F., Weintraub, S., Rogalski, E., 2013. A novel frontal pathway underlies verbal fluency in primary progressive aphasia. Brain 136, 2619–2628.

Chamberland, M., Raven, E.P., Genc, S., Duffy, K., Descoteaux, M., Parker, G.D., Tax, C. M.W., Jones, D.K., 2019. Dimensionality reduction of diffusion MRI measures for improved tractometry of the human brain. Neuroimage 200, 89–100.

Cheng, H.u., Wang, Y., Sheng, J., Sporns, O., Kronenberger, W.G., Mathews, V.P., Hummer, T.A., Saykin, A.J., 2012. Optimization of seed density in DTI tractography for structural networks. J. Neurosci. Methods 203 (1), 264–272.

Davtian, M., Ulmer, J.L., Mueller, W.M., Gaggl, W., Mulane, M.P., Krouwer, H.G., 2008. The superior longitudinal fasciculus and speech arrest. J. Comput. Assist. Tomogr. 32 (3), 410–414.

Dick, A.S., Garic, D., Graziano, P., Tremblay, P., 2019. The frontal aslant tract (FAT) and its role in speech, language and executive function. Cortex 111, 148–163.

Galantucci, S., Tartaglia, M.C., Wilson, S.M., Henry, M.L., Filippi, M., Agosta, F., Dronkers, N.F., Henry, R.G., Ogar, J.M., Miller, B.L., Gorno-Tempini, M.L., 2011. White matter damage in primary progressive aphasias: a diffusion tensor tractography study. Brain 134, 3011–3029.

Gatto, R.G., 2020. Molecular and microstructural biomarkers of neuroplasticity in neurodegenerative disorders through preclinical and diffusion magnetic resonance imaging studies. J Integr Neurosci 19, 571–592.

Gatto, R.G., Amin, M.Y., Deyoung, D., Hey, M., Mareci, T.H., Magin, R.L., 2018. Ultra-High Field Diffusion MRI Reveals Early Axonal Pathology in Spinal Cord of ALS mice. Translational Neurodegeneration 7, 20.

Gatto, R.G., Weissmann, C., Amin, M., Angeles-López, Q.D., García-Lara, L., Castellanos, L.C.S., Deyoung, D., Segovia, J., Mareci, T.H., Uchitel, O.D., Magin, R.L., 2021. Evaluation of early microstructural changes in the R6/1 mouse model of Huntington's disease by ultra-high field diffusion MR imaging. Neurobiol. Aging 102, 32–49.

Gatto, R.G., Ye, A.Q., Colon-Perez, L., Mareci, T.H., Lysakowski, A., Price, S.D., Brady, S. T., Karaman, M., Morfini, G., Magin, R.L., 2019. Detection of axonal degeneration in a mouse model of Huntington's disease: comparison between diffusion tensor imaging and anomalous diffusion metrics. Magma 32 (4), 461–471.

Golbe, L.I., Ohman-Strickland, P.A., 2007. A clinical rating scale for progressive supranuclear palsy. Brain 130, 1552–1565.

Gorno-Tempini, M.L., Brambati, S.M., Ginex, V., Ogar, J., Dronkers, N.F., Marcone, A., Perani, D., Garibotto, V., Cappa, S.F., Miller, B.L., 2008. The logopenic/phonological variant of primary progressive aphasia. Neurology 71 (16), 1227–1234.

Greenland, S., 2000. Principles of multilevel modelling. Int. J. Epidemiol. 29, 158–167.

Hall, D.A., Forjaz, M.J., Golbe, L.I., Litvan, I., Payan, C.A.M., Goetz, C.G., Leentjens, A.F. G., Martinez-Martin, P., Traon, A.-L., Sampaio, C., Post, B., Stebbins, G., Weintraub, D., Schrag, A., 2015. Scales to Assess Clinical Features of Progressive Supranuclear Palsy: MDS Task Force Report. Movement Disorders Clinical Practice 2 (2), 127–134.

Hana, A., Hana, A., Dooms, G., Boecher-Schwarz, H., Hertel, F., 2016. Depiction of dentatorubrothalamic tract fibers in patients with Parkinson's disease and multiple sclerosis in deep brain stimulation. BMC Research Notes 9, 345.

Hauw, J.J., Daniel, S.E., Dickson, D., Horoupian, D.S., Jellinger, K., Lantos, P.L., McKee, A., Tabaton, M., Litvan, I., 1994. Preliminary NINDS neuropathologic criteria for Steele-Richardson-Olszewski syndrome (progressive supranuclear palsy). Neurology 44, 2015-2019.

Höglinger, G.U., Respondek, G., Stamelou, M., Kurz, C., Josephs, K.A., Lang, A.E., Mollenhauer, B., Müller, U., Nilsson, C., Whitwell, J.L., Arzberger, T., Englund, E., Gelpi, E., Giese, A., Irwin, D.J., Meissner, W.G., Pantelyat, A., Rajput, A., van Swieten, J.C., Troakes, C., Antonini, A., Bhatia, K.P., Bordelon, Y., Compta, Y., Corvol, J.-C., Colosimo, C., Dickson, D.W., Dodel, R., Ferguson, L., Grossman, M., Kassubek, J., Krismer, F., Levin, J., Lorenzl, S., Morris, H.R., Nestor, P., Oertel, W.H., Poewe, W., Rabinovici, G., Rowe, J.B., Schellenberg, G.D., Seppi, K., van Eimeren, T., Wenning, G.K., Boxer, A.L., Golbe, L.I., Litvan, I., 2017. Clinical diagnosis of progressive supranuclear palsy: The movement disorder society criteria. Movement disorders : official journal of the Movement Disorder Society 32 (6), 853–864.

Hokelekli, F.O., Duffy, J.R., Clark, H.M., Utianski, R.L., Botha, H., Ali, F., Stierwalt, J.A., Machulda, M.M., Reichard, R.R., Dickson, D.W., Whitwell, J.L., Josephs, K.A., 2022. Autopsy Validation of Progressive Supranuclear Palsy-Predominant Speech/Language Disorder Criteria. Mov. Disord. 37 (1), 213–218.

Jeurissen, B., Descoteaux, M., Mori, S., Leemans, A., 2019. Diffusion MRI fiber tractography of the brain. NMR Biomed 32, e3785.

Josephs, K.A., Boeve, B.F., Duffy, J.R., Smith, G.E., Knopman, D.S., Parisi, J.E., Petersen, R.C., Dickson, D.W., 2005. Atypical progressive supranuclear palsy underlying progressive apraxia of speech and nonfluent aphasia. Neurocase 11 (4), 283–296.

Josephs, K.A., Duffy, J.R., Clark, H.M., Utianski, R.L., Strand, E.A., Machulda, M.M., Botha, H., Martin, P.R., Pham, N.T.T., Stierwalt, J., Ali, F., Buciuc, M., Baker, M., Fernandez De Castro, C.H., Spychalla, A.J., Schwarz, C.G., Reid, R.I., Senjem, M.L., Jack, C.R., Lowe, V.J., Bigio, E.H., Reichard, R.R., Polley, E.J., Ertekin-Taner, N., Rademakers, R., DeTure, M.A., Ross, O.A., Dickson, D.W., Whitwell, J.L., 2021. A molecular pathology, neurobiology, biochemical, genetic and neuroimaging study of progressive apraxia of speech. Nat. Commun. 12, 3452.

Josephs, K.A., Duffy, J.R., Strand, E.A., Machulda, M.M., Senjem, M.L., Lowe, V.J., Jack Jr., C.R., Whitwell, J.L., 2013. Syndromes dominated by apraxia of speech show distinct characteristics from agrammatic PPA. Neurology 81, 337–345.

Josephs, K.A., Duffy, J.R., Strand, E.A., Whitwell, J.L., Layton, K.F., Parisi, J.E., Hauser, M.F., Witte, R.J., Boeve, B.F., Knopman, D.S., Dickson, D.W., Jack Jr., C.R., Petersen, R.C., 2006. Clinicopathological and imaging correlates of progressive aphasia and apraxia of speech. Brain 129, 1385–1398.

Josephs, K.A., Whitwell, J.L., Dickson, D.W., Boeve, B.F., Knopman, D.S., Petersen, R.C., Parisi, J.E., Jack, C.R., 2008. Voxel-based morphometry in autopsy proven PSP and CBD. Neurobiol. Aging 29 (2), 280–289.

Karatas, M., 2009. Internuclear and supranuclear disorders of eye movements: clinical features and causes. Eur. J. Neurol. 16, 1265–1277.

Kataoka, H., Nishimori, Y., Kiriyama, T., Nanaura, H., Izumi, T., Eura, N., Iwasa, N., Sugie, K., 2019. Increased Signal in the Superior Cerebellar Peduncle of Patients with Progressive Supranuclear Palsy. Journal of movement disorders 12 (3), 166–171.

Kataoka, H., Tonomura, Y., Taoka, T., Ueno, S., 2008. Signal changes of superior cerebellar peduncle on fluid-attenuated inversion recovery in progressive supranuclear palsy. Parkinsonism Relat Disord 14 (1), 63–65.

Knake, S., Belke, M., Menzler, K., Pilatus, U., Eggert, K.M., Oertel, W.H., Stamelou, M., Höglinger, G.U., 2010. In vivo demonstration of microstructural brain pathology in progressive supranuclear palsy: a DTI study using TBSS. Movement disorders : official journal of the Movement Disorder Society 25, 1232–1238.

Kroonenberg, P.M., Oort, F.J., Stebbins, G.T., Leurgans, S.E., Cubo, E., Goetz, C.G., 2006. Motor function in Parkinson's disease and supranuclear palsy: simultaneous factor analysis of a clinical scale in several populations. BMC Med. Res. Method. 6, 26.

Kwon, H.G., Hong, J.H., Hong, C.P., Lee, D.H., Ahn, S.H., Jang, S.H., 2011. Dentatorubrothalamic tract in human brain: diffusion tensor tractography study. Neuroradiology 53 (10), 787–791.

Ling, H., Kovacs, G.G., Vonsattel, J.P.G., Davey, K., Mok, K.Y., Hardy, J., Morris, H.R., Warner, T.T., Holton, J.L., Revesz, T., 2016. Astrogliopathy predominates the earliest stage of corticobasal degeneration pathology. Brain 139 (12), 3237–3252.

Litvan, I., Agid, Y., Calne, D., Campbell, G., Dubois, B., Duvoisin, R.C., Goetz, C.G., Golbe, L.I., Grafman, J., Growdon, J.H., Hallett, M., Jankovic, J., Quinn, N.P., Tolosa, E., Zee, D.S., 1996. Clinical research criteria for the diagnosis of progressive supranuclear palsy (Steele-Richardson-Olszewski syndrome): report of the NINDS-SPSP international workshop. Neurology 47 (1), 1–9.

Madhavan, A., Schwarz, C.G., Duffy, J.R., Strand, E.A., Machulda, M.M., Drubach, D.A., Kantarci, K., Przybelski, S.A., Reid, R.I., Senjem, M.L., Gunter, J.L., Apostolova, L.G., Lowe, V.J., Petersen, R.C., Jack, C.R., Josephs, K.A., Whitwell, J.L., Zhang, B., 2016. Characterizing White Matter Tract Degeneration in Syndromic Variants of Alzheimer's Disease: A Diffusion Tensor Imaging Study. J. Alzheimers Dis. 49 (3), 633–643.

Madhavan, K.M., McQueeny, T., Howe, S.R., Shear, P., Szaflarski, J., 2014. Superior longitudinal fasciculus and language functioning in healthy aging. Brain Res. 1562, 11–22.

Mahoney, C.J., Malone, I.B., Ridgway, G.R., Buckley, A.H., Downey, L.E., Golden, H.L., Ryan, N.S., Ourselin, S., Schott, J.M., Rossor, M.N., Fox, N.C., Warren, J.D., 2013. White matter tract signatures of the progressive aphasias. Neurobiol. Aging 34 (6), 1687–1699.

Mollink, J., van Baarsen, K.M., Dederen, P.J., Foxley, S., Miller, K.L., Jbabdi, S., Slump, C.H., Grotenhuis, J.A., Kleinnijenhuis, M., van Cappellen van Walsum, A.M.,, 2016. Dentatorubrothalamic tract localization with postmortem MR diffusion tractography compared to histological 3D reconstruction. Brain Struct. Funct. 221, 3487–3501.

Montine, T.J., Phelps, C.H., Beach, T.G., Bigio, E.H., Cairns, N.J., Dickson, D.W., Duyckaerts, C., Frosch, M.P., Masliah, E., Mirra, S.S., Nelson, P.T., Schneider, J.A., Thal, D.R., Trojanowski, J.Q., Vinters, H.V., Hyman, B.T., 2012. National Institute on Aging-Alzheimer's Association guidelines for the neuropathologic assessment of Alzheimer's disease: a practical approach. Acta Neuropathol. 123 (1), 1–11.

Mori, S., van Zijl, P.C.M., 2002. Fiber tracking: principles and strategies - a technical review. NMR Biomed. 15 (7-8), 468–480.

Morris, H.R., Wood, N.W., Lees, A.J., 1999. Progressive supranuclear palsy (Steele-Richardson-Olszewski disease). Postgrad. Med. J. 75, 579–584.

Nicoletti, G., Tonon, C., Lodi, R., Condino, F., Manners, D., Malucelli, E., Morelli, M., Novellino, F., Paglionico, S., Lanza, P., Messina, D., Barone, P., Morgante, L., Zappia, M., Barbiroli, B., Quattrone, A., 2008. Apparent diffusion coefficient of the superior cerebellar peduncle differentiates progressive supranuclear palsy from Parkinson's disease. Movement disorders : official journal of the Movement Disorder Society 23 (16), 2370–2376.

Ou, S.-Q., Wei, P.-H., Fan, X.-T., Wang, Y.-H., Meng, F., Li, M.-Y., Shan, Y.-Z., Zhao, G.-G., 2021. Delineating the Decussating Dentato-rubro-thalamic Tract and Its Connections in Humans Using Diffusion Spectrum Imaging Techniques. Cerebellum 21 (1), 101–115.

Pascual, B., Funk, Q., Zanotti-Fregonara, P., Cykowski, M.D., Veronese, M., Rockers, E., Bradbury, K., Yu, M., Nakawah, M.O., Román, G.C., Schulz, P.E., Arumanayagam, A. S., Beers, D., Faridar, A., Fujita, M., Appel, S.H., Masdeu, J.C., 2021. Neuroinflammation is highest in areas of disease progression in semantic dementia. Brain 144, 1565–1575.

Paviour, D.C., Price, S.L., Stevens, J.M., Lees, A.J., Fox, N.C., 2005. Quantitative MRI measurement of superior cerebellar peduncle in progressive supranuclear palsy. Neurology 64 (4), 675–679.

Sakamoto, S., Kimura, T., Kajiyama, K., Ando, K., Takeda, M., Yoshikawa, H., 2021. Dentatorubrothalamic tract reduction using fixel-based analysis in corticobasal syndrome. Neuroradiology 63 (4), 529–538.

Schilling, K.G., Nath, V., Hansen, C., Parvathaneni, P., Blaber, J., Gao, Y., Neher, P., Aydogan, D.B., Shi, Y., Ocampo-Pineda, M., Schiavi, S., Daducci, A., Girard, G., Barakovic, M., Rafael-Patino, J., Romascano, D., Rensonnet, G., Pizzolato, M., Bates, A., Fischi, E., Thiran, J.-P., Canales-Rodríguez, E.J., Huang, C., Zhu, H., Zhong, L., Cabeen, R., Toga, A.W., Rheault, F., Theaud, G., Houde, J.-C., Sidhu, J., Chamberland, M., Westin, C.-F., Dyrby, T.B., Verma, R., Rathi, Y., Irfanoglu, M.O., Thomas, C., Pierpaoli, C., Descoteaux, M., Anderson, A.W., Landman, B.A., 2019a. Limits to anatomical accuracy of diffusion tractography using modern approaches. Neuroimage 185, 1–11.

Schilling, K.G., Yeh, F.C., Nath, V., Hansen, C., Williams, O., Resnick, S., Anderson, A.W., Landman, B.A., 2019b. A fiber coherence index for quality control of B-table orientation in diffusion MRI scans. Magn. Reson. Imaging 58, 82–89.

Schober, P., Boer, C., Schwarte, L.A., 2018. Correlation Coefficients: Appropriate Use and Interpretation. Anesth. Analg. 126 (5), 1763–1768.

Seki, M., Seppi, K., Mueller, C., Potrusil, T., Goebel, G., Reiter, E., Nocker, M., Steiger, R., Wildauer, M., Gizewski, E.R., Wenning, G.K., Poewe, W., Scherfler, C., 2018. Diagnostic potential of dentatorubrothalamic tract analysis in progressive supranuclear palsy. Parkinsonism Relat Disord 49, 81–87.

Steele, J.C., Richardson, J.C., Olszewski, J., 1964. Progressive Supranuclear Palsy. A Heterogeneous Degeneration Involving the Brain Stem, Basal Ganglia and Cerebellum with Vertical Gaze and Pseudobulbar Palsy. Nuchal Dystonia and Dementia. Arch Neurol 10, 333–359.

Surova, Y., Nilsson, M., Lätt, J., Lampinen, B., Lindberg, O., Hall, S., Widner, H., Nilsson, C., van Westen, D., Hansson, O., 2015. Disease-specific structural changes in thalamus and dentatorubrothalamic tract in progressive supranuclear palsy. Neuroradiology 57 (11), 1079–1091.

Thomas, C., Ye, F.Q., Irfanoglu, M.O., Modi, P., Saleem, K.S., Leopold, D.A., Pierpaoli, C., 2014. Anatomical accuracy of brain connections derived from diffusion MRI tractography is inherently limited. Proc. Natl. Acad. Sci. U. S. A. 111 (46), 16574–16579.

Tsuboi, Y., Slowinski, J., Josephs, K.A., Honer, W.G., Wszolek, Z.K., Dickson, D.W., 2003. Atrophy of superior cerebellar peduncle in progressive supranuclear palsy. Neurology 60 (11), 1766–1769.

Tuch, D.S., 2004. Q-ball imaging. Q-ball imaging. 52 (6), 1358–1372.

Whitwell, J.L., Avula, R., Master, A., Vemuri, P., Senjem, M.L., Jones, D.T., Jack, C.R., Josephs, K.A., 2011a. Disrupted thalamocortical connectivity in PSP: a resting-state fMRI, DTI, and VBM study. Parkinsonism Relat Disord 17 (8), 599–605.

Whitwell, J.L., Avula, R., Senjem, M.L., Kantarci, K., Weigand, S.D., Samikoglu, A., Edmonson, H.A., Vemuri, P., Knopman, D.S., Boeve, B.F., Petersen, R.C., Josephs, K. A., Jack Jr., C.R., 2010. Gray and white matter water diffusion in the syndromic variants of frontotemporal dementia. Neurology 74, 1279–1287.

Whitwell, J.L., Duffy, J.R., Strand, E.A., Machulda, M.M., Senjem, M.L., Gunter, J.L., Kantarci, K., Eggers, S.D., Jack Jr., C.R., Josephs, K.A., 2013. Neuroimaging comparison of primary progressive apraxia of speech and progressive supranuclear palsy. Eur. J. Neurol. 20, 629–637.

Whitwell, J.L., Höglinger, G.U., Antonini, A., Bordelon, Y., Boxer, A.L., Colosimo, C., van Eimeren, T., Golbe, L.I., Kassubek, J., Kurz, C., Litvan, I., Pantelyat, A., Rabinovici, G., Respondek, G., Rominger, A., Rowe, J.B., Stamelou, M., Josephs, K. A., 2017. Radiological biomarkers for diagnosis in PSP: Where are we and where do we need to be? Movement disorders : official journal of the Movement Disorder Society 32 (7), 955–971.

Whitwell, J.L., Master, A.V., Avula, R., Kantarci, K., Eggers, S.D., Edmonson, H.A., Jack Jr., C.R., Josephs, K.A., 2011. Clinical correlates of white matter tract degeneration in progressive supranuclear palsy. Arch. Neurol. 68, 753–760.

Whitwell, J.L., Schwarz, C.G., Reid, R.I., Kantarci, K., Jack, C.R., Josephs, K.A., 2014. Diffusion tensor imaging comparison of progressive supranuclear palsy and corticobasal syndromes. Parkinsonism Relat Disord 20 (5), 493–498.

Whitwell, J.L., Stevens, C.A., Duffy, J.R., Clark, H.M., Machulda, M.M., Strand, E.A., Martin, P.R., Utianski, R.L., Botha, H., Spychalla, A.J., Senjem, M.L., Schwarz, C.G., Jack, C.R., Ali, F., Hassan, A., Josephs, K.A., 2019. An Evaluation of the Progressive Supranuclear Palsy Speech/Language Variant. Mov Disord Clin Pract 6 (6), 452–461.

Whitwell, J.L., Tosakulwong, N., Botha, H., Ali, F., Clark, H.M., Duffy, J.R., Utianski, R. L., Stevens, C.A., Weigand, S.D., Schwarz, C.G., Senjem, M.L., Jack, C.R., Lowe, V.J., Ahlskog, J.E., Dickson, D.W., Josephs, K.A., 2020. Brain volume and flortaucipir analysis of progressive supranuclear palsy clinical variants. Neuroimage Clin 25, 102152.

Whitwell, J.L., Tosakulwong, N., Clark, H.M., Ali, F., Botha, H., Weigand, S.D., Sintini, I., Machulda, M.M., Schwarz, C.G., Reid, R.I., Jack, C.R., Ahlskog, J.E., Josephs, K.A., 2021. Diffusion tensor imaging analysis in three progressive supranuclear palsy variants. J. Neurol. 268 (9), 3409–3420.

Williams, D.R., de Silva, R., Paviour, D.C., Pittman, A., Watt, H.C., Kilford, L., Holton, J. L., Revesz, T., Lees, A.J., 2005. Characteristics of two distinct clinical phenotypes in pathologically proven progressive supranuclear palsy: Richardson's syndrome and PSP-parkinsonism. Brain 128, 1247–1258.

Yeh, F.-c., 2021. DSI Studio. Zenodo.

Yeh, F.-C., Panesar, S., Fernandes, D., Meola, A., Yoshino, M., Fernandez-Miranda, J.C., Vettel, J.M., Verstynen, T., 2018. Population-averaged atlas of the macroscale human structural connectome and its network topology. Neuroimage 178, 57–68.

Yeh, F.-C., Verstynen, T.D., Wang, Y., Fernández-Miranda, J.C., Tseng, W.-Y.I., 2013. Deterministic Diffusion Fiber Tracking Improved by Quantitative Anisotropy. PLoS One 8, e80713.

Yeh, F.C., Badre, D., Verstynen, T., 2016a. Connectometry: A statistical approach harnessing the analytical potential of the local connectome. Neuroimage 125, 162–171.

Yeh, F.-C., Panesar, S., Barrios, J., Fernandes, D., Abhinav, K., Meola, A., Fernandez-Miranda, J.C., 2019a. Automatic Removal of False Connections in Diffusion MRI Tractography Using Topology-Informed Pruning (TIP). Neurotherapeutics 16 (1), 52–58.

Yeh, F.C., Vettel, J.M., Singh, A., Poczos, B., Grafton, S.T., Erickson, K.I., Tseng, W.I., Verstynen, T.D., 2016b. Quantifying Differences and Similarities in Whole-Brain

White Matter Architecture Using Local Connectome Fingerprints. PLoS Comput Biol 12, e1005203.
Yeh, F.C., Wedeen, V.J., Tseng, W.Y., 2010. Generalized q-sampling imaging. IEEE Trans. Med. Imaging 29, 1626–1635.
Yeh, F.C., Zaydan, I.M., Suski, V.R., Lacomis, D., Richardson, R.M., Maroon, J.C., Barrios-Martinez, J., 2019b. Differential tractography as a track-based biomarker for neuronal injury. Neuroimage 202, 116131.
Zajac, L., Koo, B.B., Bauer, C.M., Killiany, R., Behalf Of The Alzheimer's Disease Neuroimaging, I., 2017. Seed Location Impacts Whole-Brain Structural Network Comparisons between Healthy Elderly and Individuals with Alzheimer's Disease. Brain sciences 7.
Zhang, Y.u., Walter, R., Ng, P., Luong, P.N., Dutt, S., Heuer, H., Rojas-Rodriguez, J.C., Tsai, R., Litvan, I., Dickerson, B.C., Tartaglia, M.C., Rabinovici, G., Miller, B.L., Rosen, H.J., Schuff, N., Boxer, A.L., Yang, S., 2016. Progression of Microstructural Degeneration in Progressive Supranuclear Palsy and Corticobasal Syndrome: A Longitudinal Diffusion Tensor Imaging Study. PLoS ONE 11 (6), e0157218.